26

FERMILAB
OCT 5 1998
LIBRARY

LAL-RT-98-04

Fermilab Library
0 1160 0067733 0

LAL/RT 98-04
September 1998

Laboratoire de l'Accélérateur Linéaire

Analytical Investigation on the Halo Formation in Space Charge Dominated Beams

J. Gao

Laboratoire de l'Accélérateur Linéaire
IN2P3-CNRS et Université de Paris-Sud, BP 34, F-91898 Orsay Cedex

NAME	I.D No.	M.S.

RETURN TO FERMILAB LIBRARY

Submitted to "Particle Accelerators"

U.E.R
de
l'Université Paris-Sud

Institut National
de Physique Nucléaire
et de Physique des Particules

B.P. 34 ~ Bâtiment 200 ~ 91898 ORSAY CEDEX

LAL/RT 98-04
September 1998

Analytical Investigation on the Halo Formation in Space Charge Dominated Beams

J. Gao
Laboratoire de L'Accélérateur Linéaire
IN2P3-CNRS et Université de Paris-Sud
B.P. 34, 91898 Orsay cedex, France

Abstract

In this paper we investigate the dynamical behaviours of a continuous intense charged particle beam in an acceleration and transport system. It is assumed that fermion particles, such as electron and proton, in the beam follow Fermi-Dirac statistics in the equilibrium state. Parametric resonances, chaotic motion, and halo formation in transverse direction of motion are investigated analytically. The analytical expressions for the parametric resonances and the maximum transverse position deviation, above which chaotic motion starts to occur due to transverse beam envelope oscillation, are derived. Analytical formulae for the current loss rate are established, which can be served as scaling laws and a guide in a numerical simulation based machine design.

1 Introduction

To generate, accelerate, and transport high current ion beams have become serious subjects of research since the beginning of 1940s originally related with military applications [1] [2]. Recently, high power ion beams are more and more demanded in the related possible applications such as thermonuclear energy production, transmutation of radioactive wastes, the production of tritium and the special materials,

and the conversion of plutonium [3]–[9]. One of the major challenges on the linac is to keep the machine maintenance hand-accessible which can be roughly quantified by a rule-of-thumb of the average particle loss rate < 1 nA/GeV/m [3]. The lost particles are mainly from the halo which surrounds the beam core. The origin of the halo formation has kept physicists working for years on analytical models and numerical simulations [10]–[24] (the references cited here are, of course, far from complete). Among others the particle-core model proposed by O'Connell, Wangler, Mills, and Crandall [10] is the simplest and the most explored, which illustrates many important features of the dynamics of the particles which constitute the halo with the assumption that the core has a uniform density and zero emittance. Now we summarize briefly the main results from what have been previously done numerically and theoretically on halo formations. Once there exists an envelope oscillation a parametric resonance might occur when the particle oscillation frequency is about half of that of the core oscillation (which is analytically predicted by Gluckstern [11] and numerically confirmed by, for example, Wangler et al. [12] and Ryne et al. [13]. An important result from the particle-core model is the prediction that these resonantly- driven halo particles have a maximum amplitude for a given mismatch amplitude, which is confirmed by numerical simulation studies. By making stroboscopic plot in phase space (which is first used in halo studies by Lagniel [14] [15]) one finds that there exist three distinct regions defined by a separatrix. The first is the so-called core-dominated region where particles spend most of their time inside the core. The second is a outer region, or the so-called focusing-dominated region, where particles spend most of their time outside of the core. In this paper we define the particles located in this region are halo particles. Finally, the regions surrounding two fixed points on the x axis (radial direction), one on each side of origin, where the particle oscillations are close to one half of the core frequency and the above mentioned parametric resonance produces large energy transfers. The three types of particle stroboscopic trajectories in phase space are schematically illustrated in Fig. 1. For a more complete summary of what we have known about halo formation the reader is suggested to read the book written by T. Wangler [2].

The problem with the existing models is that it is not obvious to predict the particle loss rate [24]. In this paper we try to explain analytically the halo formation processes in detail, and try to estimate the halo current loss rate analytically. In section 2 we discuss the par-

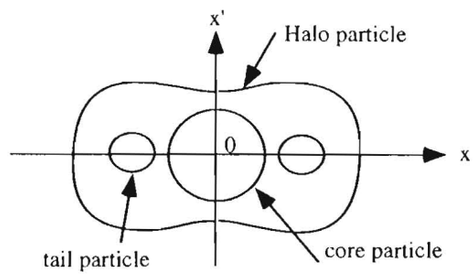

Figure 1: Schematic illustration of three types stroboscopic trajectories in phase space. The particles located in the focusing-dominated region are defined as halo particles.

ticle density distribution for a round continuous beam in a continuous solenoid focusing channel. The fermion particles, such as electron and proton, which constitute the beam are assumed to follow Fermi-Dirac statistics in the equilibrium state. In sections 3 and 4 we investigate the transverse motions of the particles originally located in the quasi-uniform density and nonuniform density regions, respectively. The conditions under which parametric resonances and the chaotic motions in both regions are established analytically. In section 5 analytical estimation of the halo particle loss rate is given and analytical current loss rate formulae are established. Finally, in section 6 we give the conclusion. The mathematical details are presented in appendices A and B.

2 Particle density distribution

To transport a space-charge limited intense current beam an optical focusing elements have to be installed along the beam line. The single particle motion in the beam is determined by the applied focusing force and the space charge force. Apparently, to establish equations for the single particle and the collective motions in a consistent way is not obvious since it depends on the concrete particle distribution. In 1950s Kapchinskij and Vladimirskij studied a "perfect beam" (but

not realistic) which has uniformly filled projection ellipses and they derived the envelope and single particle transverse motion differential equations for a continuous beam as follows (we limit ourselves to round and continuous beams) [25]:
- Envelope equation:

$$\frac{d^2R}{dz^2} + \omega_0^2 R - \frac{K}{R} - \frac{\epsilon^2}{R^3} = 0 \tag{1}$$

where R is the beam envelope in a continuous solenoid focusing channel, $K = 2(I_b/I_0)/(\beta\gamma)^3$, $\pi\epsilon$ is the beam unnormalized transverse emittance, γ and β are the normalized particle's energy and velocity (v/c), respectively, I_b is the beam current, and $I_0 = 4\pi\epsilon_0\pi m_0 c^3/q$ with m_0/q being the mass charge ratio of the particle ($I_0 = 1.7 \times 10^4$ A for electron).
- Single particle equations:

$$\frac{d^2x}{dz^2} + \left(\omega_0^2 - \frac{K}{R^2}\right) x = 0 \tag{2}$$

when $x < R$, and

$$\frac{d^2x}{dz^2} + \omega_0^2 x - \frac{K}{x} = 0 \tag{3}$$

when $x > R$. Since the KV envelope equation is derived from a specific microcanonical distribution, the validity for the other kinds of distribution is not automatic. According to Lapostolle [26] and Sacherer [27], one can use the same form of envelope equation for any possible particle distributions provided that the envelope and the emittance are defined as

$$R^2 = 4\overline{x^2} \tag{4}$$

$$\epsilon = 4\sqrt{\overline{x^2}\,\overline{x'^2} - \overline{xx'}^2} \tag{5}$$

From now on the form of the envelope equation expressed in eq. 1 is regarded as particle density distribution independent. Now we distinguish two cases: the matched and mismatched beams. Considering now a continuous focusing channel, for the first case one means:

$$\omega_0^2 R - \frac{K}{R} - \frac{\epsilon^2}{R^3} = 0 \tag{6}$$

and

$$\frac{d^2x}{dz^2} + \omega_p^2 x = 0 \tag{7}$$

for $x < R$, where $\omega_p^2 = \epsilon^2/R^4$. For the matched case, apparently, when $\epsilon = 0$ the motions of particles within the beam envelope can be equivalent to those of particles in collision free gas of zero temperature (in this paper we consider only fermion gas such as electron and proton which have half-integral spins). For the zero emittance matched beam envelope radius, R_0, one finds $R_0 = \sqrt{K}/\omega_0$. When $\epsilon \neq 0$ the stationary envelope radius will become $R = R_0 + \delta R$. Putting this expression into eq. 1, for $\delta R << R$, one finds

$$\delta R = \frac{\epsilon^2}{2\omega_0^2 R_0^3} \tag{8}$$

From eq. 1 one knows that if R deviate a little bit from R_0 at zero emittance limit the envelope oscillates approximately like an harmonic oscillator:

$$\frac{d^2\delta R}{dz^2} + \omega_R^2 \delta R = 0 \tag{9}$$

where $\omega_R = \sqrt{2}\omega_0$ which is called the envelope oscillation frequency. Now we are at the stage to estimate the stationary particle density distribution function, $n(x)$. As noted above we regard the particles in the matched beam as the particles in a fermion gas, and in consequence, the density distribution follows Fermi-Dirac statistics:

$$n(E) = \frac{n_{E=0}}{1 + \exp\left((E - \mu)/kT\right)} \tag{10}$$

where E is the particle's energy, μ is the chemical energy of the gas, k is the Boltzmann constant, and T is the temperature of the gas. The energy of a particle is proportional to the square of its plasma oscillation amplitude and kT is proportional to the square of Debye length, λ_D. One rewrites eq. 10 as

$$n(x) = \frac{n_{x=0}}{1 + \exp\left((x^2 - R_0^2)/\lambda_D^2\right)} \tag{11}$$

where λ_D is estimated as follows:

$$\lambda_D^2 = \frac{v_{thermal}^2}{\omega_p^2} = \frac{\delta R^2 \omega_R^2}{\omega_p^2} = \frac{1}{2}\frac{\epsilon^2}{\omega_0^2 R_0^2} \tag{12}$$

or

$$\frac{\lambda_D}{R_0} = \frac{\omega_p}{\omega_R} \tag{13}$$

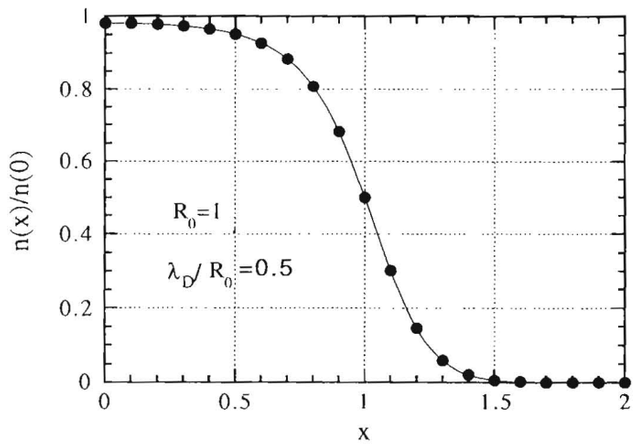

Figure 2: Stationary particle density distribution (Fermi-Dirac distribution), where $\lambda_D/R_0 = 0.5$ and $R_0 = 1$.

which is a little bit different from that found by I. Hofmann and J. Struckmeier [28]. Now we look at a more general situation when the beam is not matched with $R = R_0 + \Delta R$ and $\Delta R << R_0$. In analogy with δR we know that ΔR oscillates with envelope frequency, ω_R also. In the equilibrium state (there is no diffusion process exists) particles are assumed to follow Fermi-Dirac statistics as in the case of matched beam. The general expression for λ_D is obtained as:

$$\lambda_D^2 = \frac{v_{thermal}^2}{\omega_p^2} = \frac{(\delta R^2 + \Delta R^2)\omega_R^2}{\omega_{\Delta R}^2 + \omega_p^2} \tag{14}$$

where $\omega_{\Delta R}^2 = 2\omega_0^2 \Delta R/R_0$, ΔR and δR are statistically independent. When $\Delta R = 0$ eq. 14 reduces to eq. 12. In the case where the contribution from the definite emittance can be neglected eq. 14 can be simplified as:

$$\left(\frac{\lambda_D}{R_0}\right)^2 \approx \frac{\Delta R}{R_0} \tag{15}$$

Apparently, for a matched beam with $\epsilon = 0$ the particle density stationary distribution is uniform with an unambiguous beam radius R_0. If, however, $\lambda_D \neq 0$ there exists a nonuniform density distribution zone located near $x = R_0$ as shown in Fig. 2. To study single particle dynamics we assume that for $x < R_0 - \lambda_D$ and $x > R_0 - \lambda_D$ the particle transverse motions are described by eqs. 2 and 3, respectively. To appreciate the magnitude of the unnormalized rms emittance in a linac

we recall the analytical result from ref. 2 that after one-fourth plasma wavelength, $\lambda_p = 2\pi R_0/\sqrt{3K}$, the rms emittance of the injected beam into linac will reach a saturated value due to the charge re-distribution process:

$$\epsilon = \frac{\pi R_0}{24}\sqrt{\frac{K}{15}} \tag{16}$$

Even this result is obtained from an initially parabolic density round beam of zero emittance, it is still useful for illustrating the physical picture and the magnitude estimation. Equipped with eqs. 11, 14 and 16, one can estimate the equilibrium particle density distribution which serves as our start point for the further discussions. To summarize what we have learned from the above analysis, one assumes that for a beam constituted by fermion particles in a continuous focusing channel the stationary transverse density distribution follows Fermi-Dirac statistics. For the particles within the density quasi-uniform region they execute simple plasma oscillations. For the particles located in the nonuniform density region their dynamic behaviours are assumed to be determined by eq. 3.

The particle dynamics under envelope modulation perturbations in both regions are discussed in detail in the following two sections.

3 Instability due to parametric resonance: Arnol'd tongues

In a continuous focusing channel the particles in the quasi-uniform density region of a matched beam is shown to execute simple plasma oscillations. The question now is what will happen to these particles if the beam envelope is modulated due to either periodic focusing channel or mismatch? In this section a mismatched beam in a continuous focusing channel is considered since for a matched periodic focusing channel the procedure to treat the problem is the same. From eq. 2 it is found that if the beam envelope is modulated from the matched radius, R_0, by $\Delta R_c(z)$, the differential equation of motion reads:

$$\frac{d^2x}{dz^2} + \left(\omega_p^2 + \frac{2K}{R_0^3}\Delta R_c(z)\right)x = 0 \tag{17}$$

where $\Delta R_c(z) = \Delta R_c(z + L_c)$, and L_c is the envelope modulation period. If $\Delta R_c(z)$ is expressed as a sinusoidal function of longitudinal

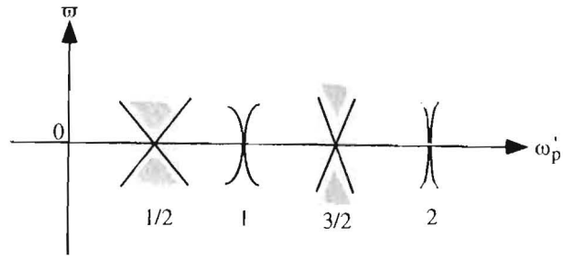

Figure 3: The shaded areas (Arnol'd tongues) correspond to the parametric resonance regions.

position, z, the stability region of x will be determined by Mathieu equation [1]. Not sticking to the mathematic rigor we assume that $\Delta R_c(z)$ is approximated by: $\Delta R_c(z) = \Delta R_{c0}$ when $0 \leq z < L_c/2$ and $\Delta R_c(z) = -\Delta R_{c0}$ when $L_c/2 \leq z < L_c$. Defining

$$\omega_p' = \frac{L_c}{2\pi}\omega_p \tag{18}$$

and

$$\varpi = \left(\frac{L_c}{2\pi}\right)^2 \frac{2K\Delta R_{c0}}{R_0^3} \tag{19}$$

one gets the stable and the parametric resonance regions described by the functions [29]:

$$\omega_p' \approx n \pm \frac{\varpi^2}{\sqrt{8}n^3}, n = 1, 2, 3, \cdots \tag{20}$$

and

$$\omega_p' \approx k/2 + \frac{2\sqrt{2}\varpi}{\pi k^2}, k = 1, 3, 5, \cdots \tag{21}$$

For $k = 1$ we obtain the result obtained by Gluckstern [11] that when the particle frequency is about one half the core frequency the parametric resonance occurs. In this paper we generalize this particular conclusion to a more general one: *when the particle frequency is about an integer times one half the core frequency the parametric resonance occurs.* The instability regions (Arnol'd tongues) are schematically illustrated in Fig. 3 by the shaded areas. From eqs. 20 and 21 one knows that the widths of the instability regions decrease with increasing resonance orders, and that the lower order resonances are

much more dangerous than the higher ones. What is very important to note is that when the resonance condition is satisfied the amplitudes of all the particles in the quasi-uniform density region increase at the same time, in consequence, the envelope radius increases until the resonance state is broken. This means that parametric resonance can induce larger amplitude core oscillation (starting from an initially small envelope oscillation) which will have a severe consequence on the motions of the particles located outside the core (quasi-uniform density region) as we will see in the next section. To avoid parametric resonance the beam parameter has to be chosen carefully. It is found that the beam unnormalized emittance ϵ should satisfy the following relation:

$$\epsilon < \epsilon^* = \sqrt{\frac{K}{2}} R_0 \tag{22}$$

The practical implication of ϵ^* is that the resultant emittance coming from the ion source and the space-charge effect shown in eq. 16 should be less than ϵ^*.

4 The onset of halo due to nonlinear resonances and stochastic motions

From what discussed in section 2 one knows that the number of the particles originally located in the focusing-dominated region is extremely few. From now on we focus our attention to the motions of the particles originally located just near R_0 and show how these particles can finally diffuse into the focusing-determined region due to beam envelope oscillation. As we have assumed in section 2 the trajectory of a particle located in the nonuniform density region is determined by eq. 3. If we define $x = R_0 + \Delta x$, where $\Delta x \ll R_0$, one finds Δx satisfies the following nonlinear differential equation:

$$\frac{d^2\Delta x}{dz^2} + \omega_0^2 \Delta x + \frac{K}{R_0}\Delta x$$
$$-\frac{K}{R_0}\left(\left(\frac{\Delta x}{R_0}\right)^2 - \left(\frac{\Delta x}{R_0}\right)^3 + \left(\frac{\Delta x}{R_0}\right)^4 - \cdots\right) = 0 \tag{23}$$

It has been shown numerically that the solution of Δx is stable and periodical [10] [14]. Now let's consider the case when there is an envelope modulation, ΔR, around R_0 due to either periodic focusing or

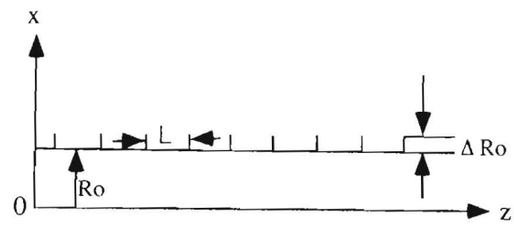

Figure 4: The envelope variation.

mismatching. The differential equation governing the particle motion near R_0 turns out to be:

$$\frac{d^2\Delta x}{dz^2} + \omega_0^2\Delta x + \frac{K}{R_0}\Delta x - \frac{K}{R_0}\left(\left(\frac{\Delta x}{R_0}\right)^2 - \left(\frac{\Delta x}{R_0}\right)^3 + \cdots\right) + \frac{K\Delta R}{R_0^2}\left(\frac{\Delta x}{R_0}\right)^2 - \cdots = 0 \tag{24}$$

For the matched case ΔR_{match} has the same period as that of the periodic focusing lattice, L. In this section we discuss only the matched periodic focusing channel, and denote $\Delta R_{match} = \Delta R_0$. To simplify the mathematics treatments we assume that $\Delta R_0(z)$ is represented by a periodic delta function of period L and amplitude ΔR_0 as shown in Fig. 4. It is shown (see appendix A) that under the periodic envelope oscillation perturbation if the amplitude of a particle's deviation Δx is larger than some limit, say Δx_{max}, the motion of this particle will become chaotic, and Δx_{max} is analytically expressed as follows:

$$\Delta x_{max} = \left(\frac{16R_0^8}{9L^2K^2\Delta R_0\beta(z)^2}\right)^{1/3} \tag{25}$$

where $\beta(z)$ is the beta function of the focusing channel. To appreciate quantitatively Δx_{max} expressed in eq. 25 we consider a continuous proton beam of $I_b = 5$A (in the practical sense, I_b is peak current for a long bunch), $R_0 = 0.005$m, $\Delta R_0 = 0.002$m, $L = 5$m, $\beta(z) = 8$m, and plot in Fig. 5 $\Delta x_{max}/R_0$ vs the beam kinetic energy, W(MeV). It is clear that no matter how strong the focusing is there exists always random moving particles at the low energy part of the linac if definite envelope oscillation presents.

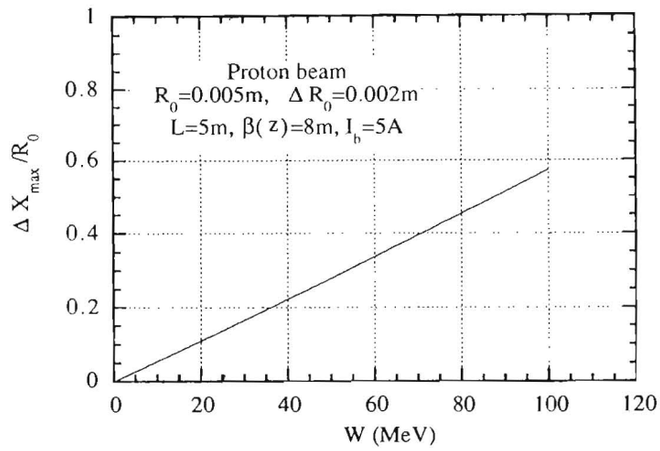

Figure 5: $\Delta X_{max}/R_0$ vs the energy of a proton beam of $I_b = 5$A, $R_0 = 0.005$m, $\Delta R_0 = 0.002$m, $L = 5$m, and $\beta(z) = 8$m.

5 Estimation of beam current loss rate

The questions now are what will be the dynamic behaviour of a particle executing random motion and how it contributes to the halo formation. According to the discussion given in appendix B one knows that the particles located near R_0 ($x = R_0 + \Delta x$) with $\Delta x \geq \Delta x_{max}$ will diffuse outwards into the focusing-dominated region and contribute to the halo. The random motions of these particles can be described by a possibility function which satisfies the Fokker-Planck equation and the diffusion coefficient is obtained analytically.

In this paper we propose two different ways to appreciate and estimate two beam loss rates. The first beam loss rate we are going to discuss is the average beam loss rate on the mechanical boundary of the beam transport system, which has an apparent practical meaning. We may make a rough estimation in the following way. From appendix B it is known that the particles located in $\Delta x \geq \Delta x_{max}$ will diffuse outwards. The current, I_d, which participates this diffusion process can be calculated as:

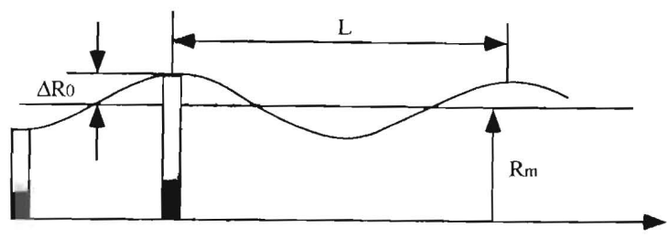

Figure 6: Schematic illustration of halo particle loss at the mechanical boundary.

$$I_d = \frac{I_b}{R_0^2}\int_{x=R_0+\Delta x_{max}}^{x=\infty} \frac{1}{1+\exp\left(\frac{x^2-R_0^2}{\lambda_D^2}\right)} dx^2$$

$$= I_b \frac{\lambda_D^2}{R_0^2} \ln\left(\frac{\exp\left((x^2-R_0^2)/\lambda_D^2\right)}{1+\exp\left((x^2-R_0^2)/\lambda_D^2\right)}\right)\Big|_{x=R_0+\Delta x_{max}} \qquad (26)$$

One can imagine that a uniform halo disk is formed around the beam core started from $x = R_0 + \Delta x_{max}$. Due to the beam envelope oscillation the dimension of the disk, which extends to the radius, R_m, of the mechanical aperture of the transport system, oscillates with $x = R_m \pm \Delta R_0$. Obviously, the particles located in $R_m \leq x \leq R_m + \Delta R_0$ are lost, as shown schematically in Fig.6, and this loss will be filled through the diffusion process. If the particle redistribution distance, or the so-called relaxation distance $\lambda_p/4$ [2], is shorter than the envelope oscillation period, the beam current loss rate, $\mathcal{R}$(A/m), can be estimated as the $\mathcal{R} = I_d(\Delta R_0/R_m)^2/L$, where $R_m >> R_0$. If, however, the relaxation distance is longer than L, one has $\mathcal{R} = 4I_d(\Delta R_0/R_m)^2/\lambda_p$. To summarize, we give a simplified beam current loss rate formula as follows:

$$\mathcal{R} \approx I_b f \frac{\Delta R_0^3}{\mathcal{L} R_0 R_m^2} \ln\left(\frac{1+\exp\left(2\Delta x_{max}/\Delta R_0\right)}{\exp\left(2\Delta x_{max}/\Delta R_0\right)}\right) \qquad (27)$$

where $\mathcal{L} = L$ when $L \geq \lambda_p/4$, $\mathcal{L} = \lambda_p$ when $L \leq \lambda_p/4$, and f is the ratio of the average beam current with respect to the peak bunch

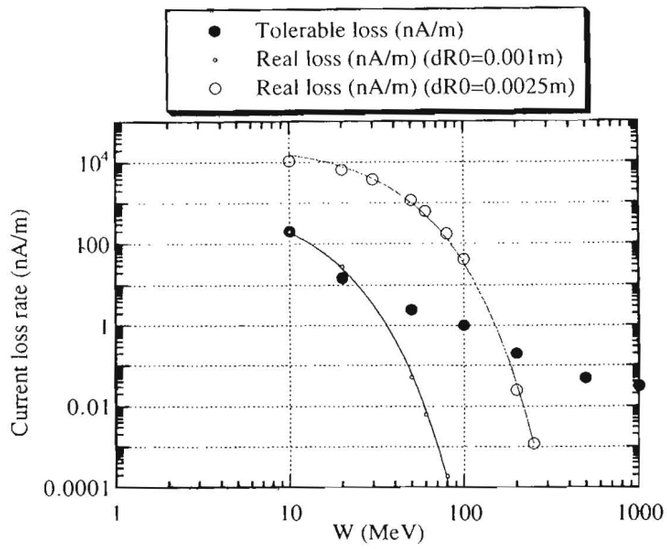

Figure 7: The current loss rates vs the energy of a proton beam of $I_b = 1A$, $R_0 = 0.005$m, $R_m = 10R_0$, $f = 0.1$, $L = 5$m, and $\beta(z) = 8$m.

current. Even the current loss rate described by eq. 27 is a somewhat pessimistic value, it can be used as a kind of scaling law and as a guide in a numerical simulation based practical machine design. In Fig. 7 we give an example to show how one can use eqs. 25 and 27 to estimate the current loss and how this current loss varies with beam parameters, where we choose $R_0 = 0.005$m, $I_b = 1$A, $f = 0.1$, $L = 5$m, $\beta(z) = 8$m, $\Delta R_0 = 0.0025$m and $\Delta R_0 = 0.001$m, respectively. In the figure the tolerable current loss rate [32] [33] is presented by the dark dots, and it is obvious that in this case ΔR_0 should be less than 0.001m.

As for the second beam loss rate, we regard the particles diffused into the focusing-dominated region as being "lost". In the following we are interested in the current loss rate in this sense. Extrapolating from what is learnt from the numerical simulations one concludes that when $\Delta x \geq \Delta x_{separatrix} \approx 2\Delta R_0$, the particle locates in the focusing-dominated region. For example, if $R_0 = 1$, $\Delta R_0 = 0.5$ then the particles with $\Delta x \geq 1$ are located in the focusing-dominated region [10]. From section 4 one knows that the particles located in

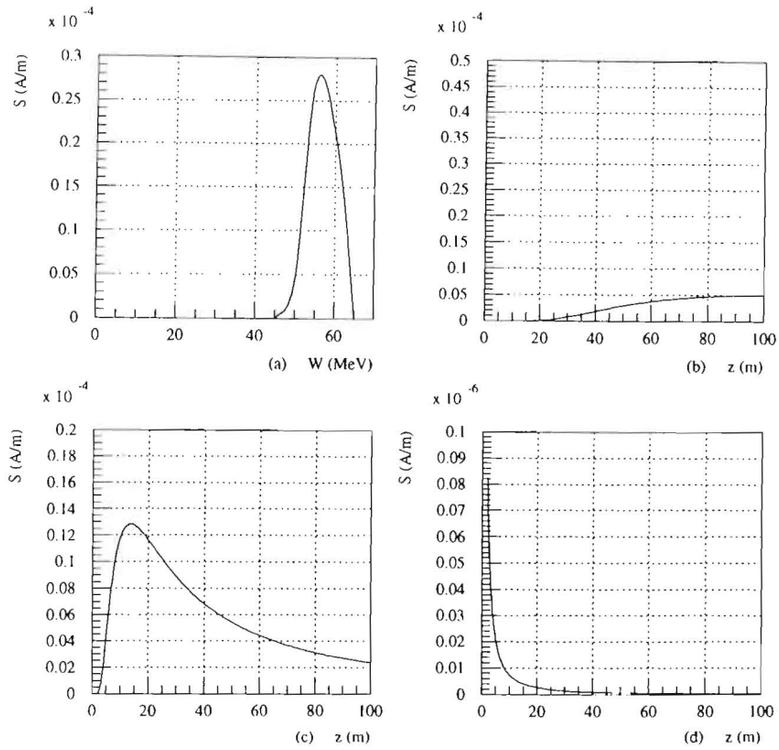

Figure 8: For a proton beam of $I_b = 1$A, $R_0 = 0.005$m, $\Delta R_0 = 0.0025$m, $f = 0.1$, $L = 5$m, and $\beta(z) = 8$m, we show how the current loss rate $\mathcal{S}$ varies with beam energy, W, and distance, z. (a) The current loss rate $\mathcal{S}$ vs the beam energy at $z - z' = 1$m. (b) $\mathcal{S}$ vs the downstream distance (no acceleration) for $W = 30$MeV . (c) $\mathcal{S}$ vs the downstream distance (no acceleration) for $W = 45$MeV. (d) $\mathcal{S}$ vs the downstream distance (no acceleration) for $W = 65$MeV.

$\Delta x_{max} \leq \Delta x \leq 2\Delta R_0$ will diffuse into the focusing-dominated region and contribute to the halo populations, and one finds (see appendix B) that the loss rate can be approximately expressed as follows:

$$\mathcal{S}(z, I|z', I') = \frac{I_r f(I - I')}{\sqrt{2\pi \mathcal{D}^*(z - z')}(z - z')} \exp\left(-\frac{(I - I')^2}{2\mathcal{D}^*(z - z')}\right) \tag{28}$$

where

$$I = \frac{9(I_b/I_0)\beta(z)L}{R_0^4(\beta\gamma)^3}\Delta R_0^2 \tag{29}$$

$$I' = \frac{9(I_b/I_0)\beta(z)L}{4R_0^4(\beta\gamma)^3}\Delta x_{max}^2 \tag{30}$$

$$\mathcal{D}^* = \mathcal{D}|_{\Delta x=\Delta x_{max}} = \frac{1}{2L} \tag{31}$$

$$I_r = I_b \frac{\lambda_D^2}{R_0^2} \ln \left(\frac{1+\exp\left((x^2-R_0^2)/\lambda_D^2\right)}{\exp\left((x^2-R_0^2)/\lambda_D^2\right)} \right) |_{x=R_0+\Delta x_{max}}^{x=R_0+2\Delta R_0} \tag{32}$$

The physical meaning of $\mathcal{S}(z, I|z', I')$ is that the beam current loses part of it into the focusing-dominated region (due to the particles' random motions at $z = z'$) at the rate of $\mathcal{S}(z, I)$ down stream. $\mathcal{S}(z, I)$ is of importance especially when the beam is mismatched locally, say near z', and one is interested in how the loss rate varies downstream. To show the usage of eq. 28 we give some examples in Fig. 8. Considering a proton beam of $I_b = 1$A, $f = 0.1$, $R_0 = 0.005$m, $\Delta R_0 = 0.0025$m, $L = 5$m, and $\beta(z) = 8$m, Fig. 8(a) shows the loss rate $\mathcal{S}(z, I)$ varies with respect to the beam energy, W(MeV), at $z - z' = 1$m. Figs. 8(b) to 8(d) show the the current loss rate $\mathcal{S}(z, I)$ downstream (no acceleration) with the proton beam of $W = 30$MeV, $W = 45$MeV, and $W = 65$MeV, respectively. It is obvious that $\mathcal{S}(z, I)$ provides us a more detailed physical image of halo formation process. In practice, collimators are useful to sweep off halo particles, and their locations, however, should be chosen carefully. Taking the case shown in Fig. 8(b) for example, to sweep off the halo particles produced at $W = 30$MeV the collimator should be installed downstream more than 20 meters.

6 Conclusion

In this paper we have investigated analytically the halo formations in continuous beams. It is assumed that for the matched beam with definite transverse emittance the density distribution follows Fermi-Dirac statistics (for fermion particles). The conditions for the particles' transverse motions to have parametric resonances and nonlinear force induced stochastic motions are derived analytically. For the parametric resonances it is found that when the particle frequency is about an integer times one half the core frequency the parametric resonance occurs. For the nonlinear force induced stochastic motions it is shown that the particles located at $\Delta x > \Delta x_{max}$ (see eq. A-35) execute stochastic motions and diffuse away from the beam core contributing to halo particles. The number of this kind of particles can be estimated by using transverse Fermi-Dirac distribution. Finally, the way to estimate the beam current loss rate due to the transverse

halo is illustrated and analytical loss rate formulae are established. In this paper we present only the results on the transverse motion of a continuous beam and omit the discussions on the halo formation due to the longitudinal motion of a bunched beam which has been the subject of the research works in refs. 34, 35 and 36.

7 Acknowledgement

The author thanks J. Le Duff and N. Pichoff (Saclay) for the clarifying discussions and their critical comments.

References

[1] M. Reiser, *Theory and the design of charged particle beams*, John Wiley & Sons, Inc. New York, 1994.

[2] T.P. Wangler, "*Principles of rf linear accelerators*", John Wiley & Sons, Inc. New York, 1998.

[3] R.A. Jameson, "Design for low beam loss in accelerators for intense neutron source applications", Proceedings of PAC93, Washington (1993), p. 3926.

[4] H. Lengeler, "Nuclear wast transmutation using high-intensity proton linear accelerators", CERN 94-01 (1994), p. 999.

[5] Y. Yamazaki, "Design issues for high-intensity, high-energy proton accelerators", Linac96, Geneva (1996), p. 592.

[6] S.X. Fang, "New direction of the applications of intense proton linac: development of nuclear energy sources", Proceedings of the 5th Chinese Particle Accelerator Society Conference, ChengDu, China (1996), p. 131 (in Chinese).

[7] Z.X. Zhao, "Progress of researchand development of clean nuclear power system driven by accelerator in the world", *Nuclear Physics Review*, **14**, no. 2 (1997) 121 (in Chinese).

[8] M. Promé, "Major projects for the use of high power linacs", Proceedings of EPAC94, Barcelona (1996), p. 9.

[9] W.T. Weng, "Ultra-high intensity proton accelerators and their applications", Proceedings of PAC97, Vancouver, Canada, 1997.

[10] J.S. O'Connell, T.P. Wangler, R.S. Mills, and K.R. Crandall, "Beam halo formation from space charge dominated beams in uniform focusing channels", Proceedings of PAC93, Washington (1993), p. 3657.

[11] R. Gluckstern, "Analytic model for halo formation in high current ion linacs", *Phys. Rev. Letters*, **73** (1994) 1247.

[12] T.P. Wangler, R.W. Garnett, E.R. Gray, R.D. Ryne, and T.S. Wang, "Dynamics of beam halo in mismatched beams", Proceedings of the XVIII international linear accelerator conference, 26-30 August 1996, Geneva, Switzerland, p. 372.

[13] R. Ryne, S. Habib, and T.P. Wangler, "Halos of intense proton beams", Proceedings of PAC95, Chicago (1995), p. 3149.

[14] J-M. Lagniel, "On halo formation from space-charge dominated beams", *Nucl. Instr. and Meth.* **A345** (1994) 45.

[15] J-M. Lagniel, "Chaotic behaviour and halo formation from 2D space-charge dominated beams", *Nucl. Instr. and Meth.* **A345** (1994) 405.

[16] M. Reiser, "Periodic focusing of intense beams", *Particle Accelerators*, **8** (1978) 167.

[17] J. Struckmeier, J. Klabune, and M. Reiser, "On the stability and emittance growth of different particle phase-space distributions in a long magnetic quadrupole channel", *Particle Accelerators*, **15** (1984) 47.

[18] J. Struckmeier and M. Reiser, "Theoretical studies of envelope oscillations and instabilities of mismatched intense charged-particle beams in periodic focusing channels", *Particle Accelerators*, **14** (1984) 227.

[19] D.L. Bruhwiler, "Model for halo dynamics in accelerating bunched beams", Proceedings of the XVIII international linear accelerator conference, 26-30 August 1996, Geneva, Switzerland, p. 355.

[20] C. Bohn, "Transverse phase-space dynamics of mismatched charged-particle beams", *Phy. Rev. letters*, **70**, No. 7 (1993) 932.

[21] J-M. Lagniel and D. Libault, "Chaos, a source of charge re-distribution and halo formation in space-charge dominated beams", Proceedings of PAC95, Chicago (1995), p. 3235.

[22] A.A. Kolomiets, S.G. Yaramishev, P.R. Zenkevich, and A.P. Korolev, "The study of nonlinear effects influenced by space charge in high intensity linac", Proceedings of PAC95, Chicago (1995), p. 3209.

[23] N. Pichoff, "Etude théorique et expérimentale du halo d'un faisceau intense de particules chargées dans un accélérateur", Thèse, Université de Paris-Sud, Dec. 1997.

[24] M. Pabst and A.P. Letchford, "Halo simulation in realistic proton linac design", Proceedings of EPAC94, Barcelona (1996), p. 27.

[25] I. Kapchinskij and V. Vladimirskij, "Limitations of proton beam current in a strong focusing linear accelerator associated with beam space charge", Proceedings of the II Int. Conf. on High Energy Accel. CERN 1959, p. 274.

[26] P.M. Lapostolle, "Desity distribution in intense beam", Proceedings of the VII international conference on high energy accelerators, August (1969), p. 205.

[27] F.J. Sacherer, "RMS envelope equations with space charge", *IEEE Trans. Nucl. Sci.* **18** (1971) 1105.

[28] I. Hofmann and J. Struckmeier, "Generalized three-dimensional equations for the emittance and the field energy of high-current beams in periodic focusing structures", *Particle Accelerators*, **21** (1987) 69.

[29] J.L. McCauley, "An introduction to nonlinear dynamics and chaos theory", *Physica Scripta*, **T20** (1988).

[30] R.L. Stratonovich, *Topics in the theory of random noise*, Vol. 1, Gordon and Breach Science Publishers Inc., 1963.

[31] H. Risken, *The Fokker-Planck equation*, Springer, 2nd edition 1989, p. 99.

[32] A.P. Fedotov and B.P. Murin, "Towards a radiation-free linac of meson or neutron generator type", Proceedings of the 1976 Linear Accelerator Conference, p. 377.

[33] J-M. Lagniel, "Halos and chaos in space-charge dominayed beams", Proceedings of EPAC96, Barcelona (1996), p. 163.

[34] J.J. Barnard and S.M. Lund, "Theory of longitudinal beam halo in rf linacs: I. Core/test-particle formulation", Proceedings of PAC97, Vancouver, Canada, 1997.

[35] S.M. Lund, "Theory of longitudinal beam halo in rf linacs: II. Envelope-particle resonances", Proceedings of PAC97, Vancouver, Canada, 1997.

[36] J. Gao, LAL/SERA 98-120, 1998.

[37] R. Ruth, "Single particle dynamics in circular accelerators", AIP conference proceedings, No. 153, p. 150.

[38] R.Z. Sagdeev, D.A. Usikov, and G.M. Zaslavsky, *Nonlinear Physics, from the pendulum to turbulence and chaos*, harwood academic publishers, 1988.

[39] B.V. Chirikov, "A universal instability of many-dimensional oscillator systems", *Physics Reports*, **52**, No. 5 (1979) 263.

[40] V.I. Veksler, Dok. Akad. Nauk USSR **43** (1944) 346.

[41] J.M. Greene, *J. Math. Phys.* **20** (1979) 1183.

[42] J. Mathews and R.L. Walker, *Mathematical methods of physics*, W.A Benjamin, Inc. (1964), p. 231.

Appendix A

We represent eq. 24 by a corresponding Hamiltonian:

$$\mathcal{H} = H_0 - \frac{K}{3}\left(\frac{\Delta x}{R_0}\right)^3 + \frac{K}{4}\left(\frac{\Delta x}{R_0}\right)^4 + \frac{K}{3}\left(\frac{\Delta R}{R_0}\right)\left(\frac{\Delta x}{R_0}\right)^3 \tag{A-1}$$

with

$$H_0 = \frac{p^2}{2} + \frac{2\omega_0^2}{2}\Delta x^2 \tag{A-2}$$

where $p = d\Delta x/dz$, $\omega_0(z)$ and $\Delta R_0(z)$ are periodic functions satisfying the relation

$$\omega_0(z) = \omega_0(z + L) \tag{A-3}$$

$$\Delta R_0(z) = \Delta R_0(z + L) \tag{A-4}$$

Clearly, the Hamiltonian, $\mathcal{H}$, contains two parts: the linear force part, H_0, and the nonlinear force part. It is natural to consider the nonlinear part as a perturbation to H_0. For the unperturbed Hamiltonian the solution of Δx is found to be [37]:

$$\Delta x = \sqrt{\epsilon_x \beta_x(z)}\cos(\phi(z) + \phi_0) \tag{A-5}$$

with

$$\phi(z) = \int_0^z \frac{ds}{\beta_x(z)} \tag{A-6}$$

where $\beta_x(z)$ is the beta function of the focusing lattice, and ϵ_x is a constant which should not be confused with the beam emittance defined in section 2. As an essential step towards further discussion on the motions under nonlinear force perturbation, we introduce action-angle variables and the Hamiltonian expressed in these new variables becomes:

$$H_0(J, \Psi) = \frac{J}{\beta_x(z)} \tag{A-7}$$

where

$$\Psi = \int_0^z \frac{dz'}{\beta_x(z')} + \phi_0 \tag{A-8}$$

and

$$J = \frac{\epsilon_x}{2} = \frac{1}{2\beta_x(z)}\left(\Delta x^2 + \left(\beta_x(z)\Delta x' - \frac{\beta_x'\Delta x}{2}\right)^2\right) \tag{A-9}$$

Since the $H_0(J,\Psi) = J/\beta_x(z)$ is still a function of the independent variable, z, we will make another canonical transformation to freeze the new Hamiltonian:

$$\Psi_1 = \Psi + \frac{2\pi\nu}{L} - \int_0^z \frac{dz'}{\beta_x(z')} \tag{A-10}$$

$$J_1 = J \tag{A-11}$$

$$H_1 = \frac{2\pi\nu}{L} J_1 \tag{A-12}$$

Now, let's recall the relation between the last action-angle variables and the particle deviation Δx:

$$\Delta x = \sqrt{2J_1\beta_x(z)}\cos\left(\Psi_1 - \frac{2\pi\nu}{L}z + \int_0^z \frac{dz'}{\beta_x(z')}\right) \tag{A-13}$$

Before putting eq. A-13 into eq. A-1, for the mathematical convenience, the periodic function ΔR is represented by a periodic delta function of period L and amplitude ΔR_0 as shown in Fig. 4. The Hamiltonian $\mathcal{H}$ becomes

$$\mathcal{H} = H_0 - \frac{K}{3}\left(\frac{\Delta x}{R_0}\right)^3 + \frac{K}{4}\left(\frac{\Delta x}{R_0}\right)^4 + \frac{K}{3}\left(\frac{\Delta R_0}{R_0}\right)\left(\frac{\Delta x}{R_0}\right)^3 L \sum_{k=-\infty}^{\infty} \delta(z-kL) \tag{A-14}$$

Putting eq. A-13 into eq. A-14 and eliminating fast phase dependent varying terms in the second and the third terms in eq. A-14, one gets

$$\mathcal{H} = \frac{2\pi\nu}{L}J_1 + \frac{K}{4R_0^4}(2J_1\beta(z))^{4/2}\frac{1}{2^4}\frac{4!}{((4/2)!)^2}$$

$$+\frac{K}{3}\left(\frac{\Delta R_0}{R_0^4}\right)(2J_1\beta(z))^{3/2}\cos^3\Psi_1 L \sum_{k=-\infty}^{\infty} \delta(z-kL) \tag{A-15}$$

where we have used trigonometric relations:

$$\cos^m\theta\cos n\theta = 2^{-m}\sum_{r=0}^{m}\frac{m!}{(m-r)!r!}\cos(n-m+2r)\theta \tag{A-16}$$

$$\cos^3\theta = \frac{2}{2^3}(\cos 3\theta + 3\cos\theta) \tag{A-17}$$

$$\cos^4\theta = \frac{1}{2^4}(\cos 4\theta + 4\cos 2\theta + \frac{4!}{((4/2)!)^2}) \tag{A-18}$$

From Hamilton's equations

$$\frac{dJ_1}{dz} = -\frac{\partial \mathcal{H}}{\partial \Psi_1} \tag{A-19}$$

$$\frac{d\Psi_1}{dz} = \frac{\partial \mathcal{H}}{\partial J_1} \tag{A-20}$$

one gets the differential equations of motion in terms of action-angle variables:

$$\frac{dJ_1}{dz} = -\frac{K}{3}\left(\frac{\Delta R_0}{R_0^4}\right)(2J_1\beta(z_1))^{3/2}\frac{d\cos^3\Psi_1}{d\Psi_1}L\sum_{k=-\infty}^{\infty}\delta(z-kL) \tag{A-21}$$

$$\frac{d\Psi_1}{dz} = \frac{2\pi\nu}{L} + \frac{4!K\beta(z)^2}{2^5R_0^4}J_1 \tag{A-22}$$

Now it is the moment to change this differential equations to the difference equations which is *suitable* to analyse the possibilities of the onset of stochasticity [38] [39]. Since the perturbations have a natural periodicity of L we will sample the dynamic quantities at a sequence of z_i with constant interval L assuming that the characteristic time between two consecutive adiabatic invariance breakdown intervals is shorter than L/c. In fact this is exactly the stroboscopic map used firstly by Lagniel [14] in his numerical simulations on halo formations. The differential equations in eqs. A–21 and A–22 are reduced to

$$\overline{J_1} = \overline{J_1}(\Psi_1, J_1) \tag{A-23}$$

$$\overline{\Psi_1} = \overline{\Psi_1}(\Psi_1, J_1) \tag{A-24}$$

where the bar stands for the next sampled value after the corresponding unbared previous value.

$$\overline{J_1} = J_1 - \frac{K}{3}\left(\frac{\Delta R_0}{R_0^4}\right)(2J_1\beta(z_1))^{3/2}\frac{d\cos^3\Psi_1}{d\Psi_1}L \tag{A-25}$$

$$\overline{\Psi_1} = \Psi_1 + 2\pi\nu + \frac{4!K\beta(z)^2}{2^5R_0^4}\overline{J_1} \tag{A-26}$$

From the trigonometric relation, apparently, the right-hand side of eq. A–25 contains sinusoidal functions of phases, Ψ_1 and $3\Psi_1$. If the tune ν is far from the resonance lines $\nu = m/n$, where m and n are integers (n=1 and 3 for this specific problem), the invariant tori of the unperturbed motion are preserved under the presence of the small

perturbations by virtue of the Kolmogorov-Arnold-Moser (KAM) theorem. If, however, ν is close to the above mentioned resonance line, the situation is getting complicated and under some conditions the KAM invariant tori can be broken. Taking the third order resonance, $m/3$, for example, we keep only the sinusoidal function with phase $3\Psi_1$ in eq. A–25 and the dominant phase independent nonlinear term in eq. A–26, and as the result, we have eqs. A–25 and A–26 reduced to

$$\overline{J_1} = J_1 + A \sin 3\Psi_1 \tag{A–27}$$

$$\overline{\Psi_1} = \Psi_1 + B\overline{J_1} \tag{A–28}$$

with

$$A = \frac{LK\Delta R_0}{4R_0^4}(2J_1\beta(z))^{3/2} \tag{A–29}$$

$$B = \frac{3K\beta(z)^2}{4R_0^4}L \tag{A–30}$$

where we have dropped the constant phase in eq. A–26. It is helpful to transform eqs. A–29 and A–30 into the form so-called *standard mapping* [39] (the mapping firstly established in the microtron invented by Veksler [40]) expressed as

$$\overline{I} = I + K_0 \sin\theta \tag{A–31}$$

$$\overline{\theta} = \theta + \overline{I} \tag{A–32}$$

with $\theta = 3\Psi$, $I = 3BJ_1$ and $K_0 = 3AB$. By virtue of the Chirikov criterion [39] it is known that when $|K_0| \geq 0.97164$ [41] resonance overlapping occurs, stochastic motions and the diffusion process appear. Therefore,

$$|K_0| \leq 1 \tag{A–33}$$

can be taken as a natural criterion for the determination of the onset of the halo formation. Putting eqs. A–29 and A–30 into eq. A–33, one gets

$$|K_0| = \frac{9L^2K^2\beta(z)^2\Delta R_0}{16R_0^8}(2J_1\beta(z))^{3/2} \leq 1 \tag{A–34}$$

and consequently, one finds maximum stable $\Delta x(z)$ value corresponding to $m/3$ resonance:

$$\Delta x_{max} = (2J_1\beta(z))^{1/2} \leq \left(\frac{16R_0^8}{9L^2K^2\Delta R_0\beta(z)^2}\right)^{1/3} \tag{A–35}$$

Readers can easily find that for the first order resonance Δx_{max} is exactly the same expression as that described in eq. A–35. Obviously, if a particle is located at $\Delta x > \Delta x_{max}$ then this particle will execute random motion. In appendix B we discuss the behaviour of these random moving particles.

Appendix B

Now we look at the motions of those particles which do not satisfy the condition given by eq. A–33. Once a particle begins to execute stochastic motion the phase mixing occurs, and the mapping given by eqs. A–31 and A–32 can be regarded as a Markov process [30], and in consequence, the possibility distribution function $\mathcal{F}(z, I)$ satisfies the Fokker-Planck equation:

$$\frac{\partial \mathcal{F}}{\partial z} = -\frac{\partial(\mathcal{A}\mathcal{F})}{\partial I} + \frac{1}{2}\frac{\partial^2(\mathcal{D}\mathcal{F})}{\partial I^2} \tag{B–1}$$

where

$$\mathcal{A} = \frac{<< \Delta I >>}{L} \tag{B–2}$$

and

$$\mathcal{D} = \frac{<< (\Delta I)^2 >>}{L} \tag{B–3}$$

where the notation $<<>>$ denotes the average over phase θ. From eq. A–31 one knows

$$\Delta I = K_0 sin\theta \tag{B–4}$$

and obviously, one has

$$\mathcal{A} = 0 \tag{B–5}$$

and the diffusion coefficient

$$\mathcal{D} = \frac{K_0^2}{2L} \tag{B–6}$$

The solutions of the Fokker-Planck equation are discussed in detail in ref. 31. Once $\mathcal{F}$ is solved with initial condition one can calculate the probability current, $\mathcal{S}(z, I)$, defined as:

$$\mathcal{S}(z, I) = \mathcal{A}\mathcal{F} - \frac{\partial(\mathcal{D}\mathcal{F})}{\partial I} \tag{B–7}$$

Inserting eqs. B–5 and B–6 into eq. B–1 and eq. B–7 one gets

$$\frac{\partial \mathcal{F}}{\partial z} = \frac{1}{2}\frac{\partial^2(\mathcal{D}\mathcal{F})}{\partial I^2} \tag{B–8}$$

and

$$\mathcal{S}(z, I) = -\frac{\partial(\mathcal{D}\mathcal{F})}{\partial I} \tag{B–9}$$

Now, the difficulty in front of us is that $\mathcal{D}$ is a function of I. When the diffusion coefficient is very small one can use WKB method [31] to transform the problem into that of solving a first order nonlinear partial differential equation instead of solving directly eq. B–8. In this paper we simplify our task by taking $\mathcal{D}$ as a constant, $\mathcal{D}^*$, which takes the value when the particles start to move randomly, and we obtain the analytical solution of $F(z, I)$ with the initial condition $\mathcal{F}(z', I|z', I') = \delta(I - I')$ as follows [42]:

$$\mathcal{F}(z, I|z', I') = \frac{1}{\sqrt{2\pi\mathcal{D}^*(z - z')}} \exp\left(-\frac{(I - I')^2}{2\mathcal{D}^*(z - z')}\right) \tag{B–10}$$

where $\mathcal{D}^* = 1/2L$ and $z > z'$. The general solution for the possibility distribution with the initial distribution $\mathcal{W}(z', I')$ is given by

$$\mathcal{W}(z, I) = \int \mathcal{F}(z, I|z', I')\mathcal{W}(z', I')dI' \tag{B–11}$$

In the following, however, we will treat the problem in an approximate way. From section 5 we know that the particles located in $\Delta x_{max} \leq \Delta x \leq 2\Delta R_0$ will diffuse into the focusing-dominated region and contribute to the halo populations, and beam current, I_r, in $\Delta x_{max} \leq \Delta x \leq 2\Delta R_0$ can be estimated as

$$I_r = \frac{I_b}{R_0^2}\int_{x=R_0+\Delta x_{max}}^{x=R_0+2\Delta R_0} \frac{1}{1 + \exp\left(\frac{x^2 - R_0^2}{\lambda_D^2}\right)} dx^2$$

$$= I_b \frac{\lambda_D^2}{R_0^2} \ln\left(\frac{1 + \exp\left((x^2 - R_0^2)/\lambda_D^2\right)}{\exp\left((x^2 - R_0^2)/\lambda_D^2\right)}\right)\Big|_{x=R_0+\Delta x_{max}}^{x=R_0+2\Delta R_0} \tag{B–12}$$

Now we take I_r as the amplitude of the delta function used above and obtain the current loss rate from the beam tail into the focusing-dominated region as follows:

$$\mathcal{S}(z, I|z', I') = \frac{I_r f(I - I')}{\sqrt{2\pi\mathcal{D}^*(z - z')}(z - z')} \exp\left(-\frac{(I - I')^2}{2\mathcal{D}^*(z - z')}\right) \tag{B–13}$$

where $\mathcal{S}$ has the unity of A/m and is a measure of average current loss due to the factor f, the ratio of average current and the peak bunch current.